http://dx.doi.org/10.2106/JBJS.OA.19.00011

The following content was supplied by the authors as supporting material and has not been copy-edited or verified by JBJS.

Appendix 1

Definition of Points of Interest in Individual Elbow Bones

1. Distal part of the humerus

The center axis of an automatically computer-generated cylinder that approximated to the trochlea and capitellum was used. Eleven sagittal planes were determined perpendicular to the axis based on anatomical landmarks: planes passing the lateral verge of the capitellum (plane 0), greatest convexity of the capitellum (plane 2), capitello-trochlear groove (plane 4), lateral trochlear ridge (plane 6), trochlear groove (plane 8), and medial verge of the trochlea (plane 11). Planes 1, 3, 5, and 7 bisected each interval, and planes 9 and 10 trisected the interval between planes 8 and 11. Subsequently, planes, including the axis, were determined at the midpoint between the bottom of the coronoid and olecranon fossae, and its proximal direction was defined as 0° in the lateral view of the right elbow. Twelve planes, including the axis, were incremented by 30° in a clockwise direction from the 0° plane (0°, 30°, 60°, 90°, 120°, 150°, 180°, 210°, 240°, 270°, 300°, and 330° planes) (Fig. 2-A).

2.1. Trochlear notch of the proximal part of the ulna

The sagittal plane passing the coronoid and olecranon tips and the bottom of the ridge of the ulnar trochlear notch was determined as plane 8, with the plane number corresponding to the humerus counterpart. Parallel to this plane, we also determined planes 6 and 11 passing the lateral and medial verge of the anterior half of the trochlea notch, plane 7 bisecting the interval between planes 6 and 8, and planes 9 and 10 trisecting the interval between planes 8 and 11. Perpendicular to the sagittal planes, including the midpoint of coronoid and olecranon tips, the planes passing the coronoid and olecranon tips and bottom of the ridge were defined as planes C, O, and 0, respectively. Furthermore, planes C1 to C5, dividing the arc between planes 0 and C into 6 equal intervals counterclockwise, and planes O1 to O5, dividing the arc between planes 0 and O into 6 equal intervals clockwise, were determined (Fig. 2-B).

2.2. Proximal sigmoid notch of the proximal part of the ulna

We set 4 points on the corner around the articular surface of the proximal sigmoid notch and trisected each of the 4 sides divided by these points. Subsequently, 2 opposing points were connected on the diagonal side and the intersection points were determined (Fig. 2-C).

3.1. *Dish* of the radial head

The deepest point of the concavity of the *dish* articular surface was identified, and the axis defined by connecting this point and the apex of the distal radial styloid. The plane, including this axis, was also determined at the midpoint between the volar and dorsal rims of the sigmoid notch of the distal radius, and its anterior direction defined as 0° in the proximal view of the radial head in the right side. Twelve planes, including the axis, were incremented by 30° clockwise from the 0° plane (0°, 30°, 60°, 90°, 120°, 150°, 180°, 210°, 240°, 270°, 300°, and

http://dx.doi.org/10.2106/JBJS.OA.19.00011

330° planes). Subsequently, the rim circumference within the articular facet and its intersection points with 12 planes were determined[1]. The interval between the deepest point and rim was quadrisected on each plane, and the points on the same circumference (25%, 50%, 75%, and rim circumferences) were categorized. Furthermore, the area determined by 30°, 60°, 90°, 120°, and 150° planes was defined as the safe zone corresponding to the area not articulating with the proximal sigmoid notch[2-4]. The rest of the area was defined as the articular zone (Fig. 2-D).

3.2. *Side* of the radial head

Five planes were determined around the periphery of the radial head, dividing the radial head height into 6 equal intervals, and their intersections were set with the former 12 planes (Fig. 2-D).

References

1. Yeung C, Deluce S, Willing R, Johnson M, King GJ, Athwal GS. Regional variations in cartilage thickness of the radial head: implications for prosthesis design. J Hand Surg Am. 2015 Dec;40(12):2364-71.e1.
2. Giannicola G, Manauzzi E, Sacchetti FM, Greco A, Bullitta G, Vestri A, Cinotti G. Anatomical variations of the proximal radius and their effects on osteosynthesis. J Hand Surg Am. 2012 May;37(5):1015-23. Epub 2012 Mar 28.
3. Kuhn S, Burkhart KJ, Schneider J, Muelbert BK, Hartmann F, Mueller LP, et al. The anatomy of the proximal radius: implications on fracture implant design. J Shoulder Elbow Surg. 2012 Sep;21(9):1247-54. Epub 2012 Feb 9.
4. Ries C, Muller M, Wegmann K, Pfau DB, Muller LP, Burkhart KJ. Is an extension of the safe zone possible without jeopardizing the proximal radioulnar joint when performing a radial head plate osteosynthesis? J Shoulder Elbow Surg. 2015 Oct;24(10):1627-34. Epub 2015 May 1.

http://dx.doi.org/10.2106/JBJS.OA.19.00011

Appendix 2

Validation for Cartilage Thickness Measurements

Accuracy tests were conducted to validate cartilage thickness measurements.

Materials and Methods

Specimen Preparation

We analyzed 6 distal part of the humerus (samples 1–6) obtained from 3 male and 1 female cadavers embalmed in formalin. At the time of death, specimens were aged 74–95 (mean, 85.3) years. Specimens were prepared according to the procedures described in the Materials and Methods section of the manuscript. Experimental flow chart is presented as an Appendix Figure.

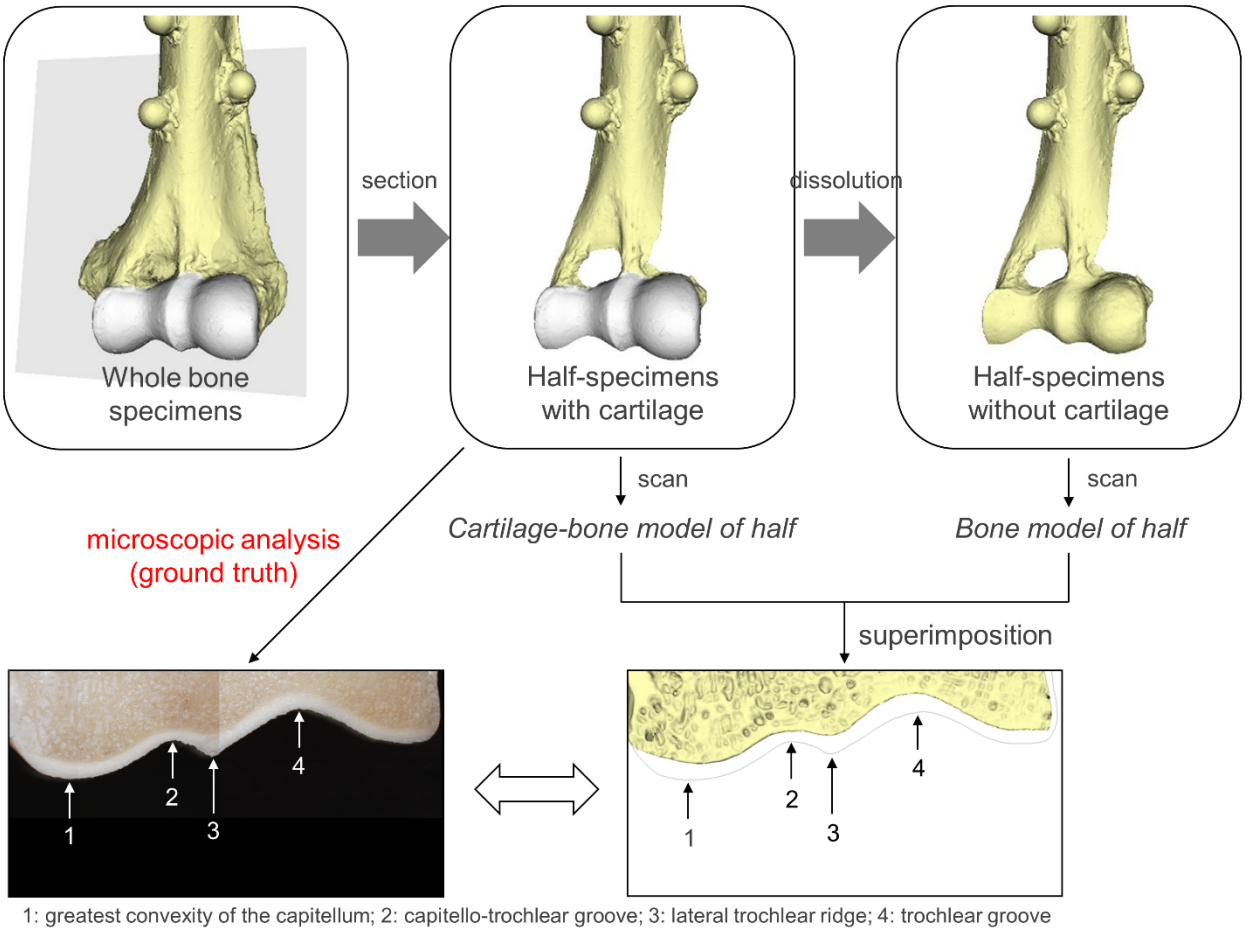

Appendix Figure Experimental flow chart

Creation of Cartilage-Bone Model of Half

http://dx.doi.org/10.2106/JBJS.OA.19.00011

All specimens were sectioned into halves such that the half-specimens had 4 steel spheres. First, in the cross-sectional plane of the specimen, with use of a stereomicroscope (AZ-100; Nikon) and a digital template, we manually measured the anatomical thickness of the articular cartilage from the cartilage surface to the chondro-osseous junction at the following anatomical landmarks: (1) greatest convexity of the capitellum, (2) capitello-trochlear groove, (3) lateral trochlear ridge, and (4) trochlear groove (Fig. 3-A). Furthermore, we assessed the intra- and interobserver reproducibility of 3 of the authors (S.M., S.A., and A.S.) for these microscopic measurements using intraclass correlation coefficients (ICCs) and the mean error of measurements. Second, each half-specimen with 4 steel spheres was scanned with use of a 3-dimensional (3-D) optical laser scanner (Rexcan CS+ 5.0 Mega pixels; Medit), and 3-D half bone models with cartilage (*cartilage-bone model of half*) were created in the corresponding proceeding software (ezScan7; Medit).

Creation of Bone Model of Half

In each half-specimen with 4 steel spheres, the articular cartilage was dissolved in the same manner as described in the Materials and Methods section of the manuscript, and the cartilage-free bones were then rescanned to create 3-D half bone models without cartilage (*bone model of half*).

Cartilage Measurements on the 3-Dimensional Model

The *cartilage-bone model of half* was superimposed onto the *bone model of half* to measure the cartilage thickness on the 3-D model with reference to the 4 steel ball registrations using the iterative closest point algorithm[1]. Cartilage thickness values were then measured at 4 anatomical landmarks on the cartilage surface by determining the step-off distance between these models.

Evaluation of Cartilage Thickness Measurements

With microscopic measurements as “ground-truth,” we validated cartilage thickness measurements in the scanned models by comparing with this ground truth using the mean percentage change and error of measurements.

Results and Conclusion

With respect to the evaluation of microscopic measurement the ICC and mean error of measurements were 0.98 and 0.044 ± 0.039 mm and 0.95 and 0.065 ± 0.063 mm for the intra-

http://dx.doi.org/10.2106/JBJS.OA.19.00011

and interobserver reproducibility, respectively, which were almost consistent with results that one of the authors previously reported[2].

Results shown in the Appendix Table showed that the mean percentage change and error of measurements were 1.80% ± 1.65% and 0.024 ± 0.017 mm, respectively. These findings should not affect the study conclusions even with these considerably small errors, and it appears justified as our measurements in the present study.

Appendix Table Cartilage thickness measurements at 4 anatomical landmarks

			Measurements	
	Percent change (%)	Error of measurements (mm)	Microscopy (mm)	Scanned model (mm)
Sample 1				
1: greatest convexity of the capitellum	0.92	0.016	1.766	1.782
2: capitello-trochlear groove	1.74	0.029	1.666	1.695
3: lateral trochlear ridge	0.18	0.004	1.982	1.986
4: trochlear groove	1.80	0.029	1.635	1.606
Sample 2				
1: greatest convexity of the capitellum	1.99	0.028	1.435	1.407
2: capitello-trochlear groove	1.80	0.030	1.671	1.641
3: lateral trochlear ridge	1.24	0.023	1.863	1.840
4: trochlear groove	1.02	0.015	1.469	1.454
Sample 3				
1: greatest convexity of the capitellum	0.07	0.001	1.354	1.355
2: capitello-trochlear groove	0.19	0.003	1.654	1.657
3: lateral trochlear ridge	0.44	0.009	1.975	1.984
4: trochlear groove	2.79	0.040	1.463	1.423
Sample 4				
1: greatest convexity of the capitellum	3.01	0.035	1.212	1.177
2: capitello-trochlear groove	4.70	0.061	1.368	1.307
3: lateral trochlear ridge	1.79	0.019	1.057	1.038
4: trochlear groove	4.25	0.046	1.126	1.080

http://dx.doi.org/10.2106/JBJS.OA.19.00011

Sample 5				
1: greatest convexity of the capitellum	0.77	0.013	1.669	1.656
2: capitello-trochlear groove	2.31	0.025	1.038	1.063
3: lateral trochlear ridge	1.13	0.022	1.921	1.899
4: trochlear groove	0.41	0.008	1.832	1.840
Sample 6				
1: greatest convexity of the capitellum	0.21	0.003	1.558	1.555
2: capitello-trochlear groove	1.38	0.018	1.294	1.276
3: lateral trochlear ridge	7.01	0.066	1.001	0.935
4: trochlear groove	2.08	0.031	1.534	1.503
Mean ± SD	1.80 ± 1.65	0.024 ± 0.017		
Median (IQR)	1.56 (0.69, 2.14)	0.022 (0.012, 0.030)		
Range	0.07−7.01	0.001−0.066		

SD, standard deviation; IQR, interquartile range

http://dx.doi.org/10.2106/JBJS.OA.19.00011

References

1. Besl P, McKay N. A method for registration of 3D shapes. IEEE Trans Patt Anal. 1992;14(2):239-56.
2. Akiyama K, Sakai T, Koyanagi J, Murase T, Yoshikawa H, Sugamoto K. Three-dimensional distribution of articular cartilage thickness in the elderly cadaveric acetabulum: a new method using three-dimensional digitizer and CT. Osteoarthritis Cartilage. 2010 Jun;18(6):795-802. Epub 2010 Mar 24.

http://dx.doi.org/10.2106/JBJS.OA.19.00011

Appendix 3

Table I Comparison of grouped cartilage thickness among *capitellum*, *intermediate* region, and *trochlea* in the distal part of the humerus (mm)

	Region			p value		
	Capitellum	*Intermediate* region	*Trochlea*	*Cap* vs. *Int*	*Cap* vs. *Tro*	*Int* vs. *Tro*
Mean ± SD	1.08 ± 0.14	1.27 ± 0.17	0.96 ± 0.16	**< 0.001** [a]	0.078 [b]	**< 0.001** [a]
Median (IQR)	1.08 (0.98, 1.22)	1.21 (1.16, 1.44)	0.89 (0.83, 1.10)			
Range	0.80−1.27	1.03−1.56	0.74−1.26			

SD, standard deviation; IQR, interquartile range; *Cap*, *Capitellum*; *Int*, *Intermediate* region; *Tro*, *Trochlea*
Statistically significant p value with Bonferroni adjustment is shown in bold ($p < 0.05$).
a indicates p value from unpaired t test.
b indicates p value from Mann-Whitney U test.

http://dx.doi.org/10.2106/JBJS.OA.19.00011

Table II Comparison of subgrouped cartilage thickness among *anterior*, *inferior*, and *posterior* zones in the distal part of the humerus (mm)

	Region			p value		
	Anterior zone	*Inferior* zone	*Posterior* zone	*Ant* vs. *Inf*	*Ant* vs. *Pos*	*Inf* vs. *Pos*
Capitellum						
Mean ± SD	1.02 ± 0.14	1.22 ± 0.18	0.65 ± 0.25	**< 0.001** [a]	**< 0.001** [a]	**< 0.001** [a]
Median (IQR)	1.05 (0.88, 1.13)	1.23 (1.14, 1.36)	0.67 (0.48, 0.79)			
Range	0.83−1.24	0.87−1.47	0.24−1.11			
Intermediate region						
Mean ± SD	1.34 ± 0.16	1.40 ± 0.24	1.06 ± 0.18	> 0.999 [b]	**< 0.001** [a]	**< 0.001** [b]
Median (IQR)	1.36 (1.23, 1.46)	1.28 (1.20, 1.68)	1.00 (0.95, 1.22)			
Range	1.04−1.61	1.14−1.82	0.68−1.37			
Trochlea						
Mean ± SD	0.91 ± 0.15	1.12 ± 0.20	0.82 ± 0.16	**0.006** [b]	0.273 [b]	**< 0.001** [b]
Median (IQR)	0.87 (0.81, 1.01)	1.08 (0.94, 1.30)	0.79 (0.70, 0.95)			
Range	0.63−1.18	0.87−1.45	0.63−1.11			

SD, standard deviation; IQR, interquartile range; *Ant*, *Anterior* zone; *Int*, *Inferior* zone; *Pos*, *Posterior* zone
Statistically significant p value with Bonferroni adjustment is shown in bold ($p < 0.05$).
a indicates p value from unpaired t test.
b indicates p value from Mann-Whitney U test.

http://dx.doi.org/10.2106/JBJS.OA.19.00011

Table III Partial correlation analysis for cartilage thickness variation of the proximal part of the ulna

	n	*r*	p value
Trochlear notch			
Coronoid			
planes C1 to C5	492	0.39	< 0.001
planes 6 to 11	492	−0.45	< 0.001
Olecranon			
planes O1 to O5	444	0.11	0.016
planes 6 to 10	444	0.03	0.483
Proximal sigmoid notch			
PA1-PA4	317	0.64	< 0.001
PD1-PD4	317	−0.73	< 0.001

n, number of points used in the analysis
r, partial Pearson correlation coefficient
Coronoid: posterior-anterior in planes C1 to C5, lateral-medial in planes 6 to 11
Olecranon: distal-proximal in planes O1 to O5, lateral-medial in planes 6 to 10
Proximal sigmoid notch: posterior-anterior in PA1-PA4, proximal-distal in PD1-PD4
Strength of association: slight (r < 0.2), low (r = 0.2–0.4), moderate (r = 0.4–0.7), high (r > 0.7)

http://dx.doi.org/10.2106/JBJS.OA.19.00011

Table IV Comparison of cartilage thickness circumferences of the radial head (*Dish*) (mm)

	Circumference					p value									
	Deepest	25%	50%	75%	Rim	Deepest vs. 25%	Deepest vs. 50%	Deepest vs. 75%	Deepest vs. Rim	25% vs. 50%	25% vs. 75%	25% vs. Rim	50% vs. 75%	50% vs. Rim	75% vs. Rim
Mean ± SD	0.73 ± 0.15	0.73 ± 0.16	0.77 ± 0.14	0.86 ± 0.14	1.10 ± 0.17	> 0.999 [a]	> 0.999 [a]	0.073 [a]	**< 0.001 [a]**	> 0.999 [a]	0.085 [a]	**< 0.001 [a]**	0.455 [a]	**< 0.001 [a]**	**< 0.001 [a]**
Median (IQR)	0.75 (0.65, 0.81)	0.76 (0.66, 0.82)	0.79 (0.68, 0.87)	0.90 (0.80, 0.96)	1.15 (0.96, 1.22)										
Range	0.45–1.06	0.43–1.05	0.47–1.03	0.56–1.03	0.74–1.34										

SD, standard deviation; IQR, interquartile range
Statistically significant p value with Bonferroni adjustment is shown in bold ($p < 0.05$).
a indicates p value from unpaired t test.
b indicates p value from Mann-Whitney U test.

http://dx.doi.org/10.2106/JBJS.OA.19.00011

Table V Comparison of cartilage thickness circumferences of the radial head (*Side*) (mm)

	Circumference					p value									
	Level 1	Level 2	Level 3	Level 4	Level 5	Level 1 vs. 2	Level 1 vs. 3	Level 1 vs. 4	Level 1 vs. 5	Level 2 vs. 3	Level 2 vs. 4	Level 2 vs. 5	Level 3 vs. 4	Level 3 vs. 5	Level 4 vs. 5
Mean ± SD	1.02 ± 0.17	0.71 ± 0.15	0.52 ± 0.11	0.42 ± 0.09	0.28 ± 0.07	< **0.001** [a]	< **0.001** [a]	< **0.001** [a]	< **0.001** [a]	< **0.001** [a]	< **0.001** [a]	< **0.001** [a]	**0.021** [a]	< **0.001** [a]	< **0.001** [a]
Median (IQR)	1.06 (0.88, 1.14)	0.74 (0.60, 0.84)	0.51 (0.44, 0.61)	0.44 (0.37, 0.46)	0.28 (0.23, 0.33)										
Range	0.73−1.32	0.41−0.92	0.31−0.73	0.27−0.58	0.14−0.41										

SD, standard deviation; IQR, interquartile range
Statistically significant p value with Bonferroni adjustment is shown in bold ($p < 0.05$).
a indicates p value from unpaired t test.
b indicates p value from Mann-Whitney U test.